Macromolecular Materials and Engineering
Open Access
www.mame-journal.de

Effect of *Tulbaghia violacea*-Derived Devulcanized Rubber on the Properties of Natural Rubber/Styrene-Butadiene Rubber Blends

*Jabulani I. Mnyango, Buyiswa G. Hlangothi, Briswell Mabuto, Christopher D. Woolard, and Shanganyane P. Hlangothi**

The current study serves to demonstrate the potential utilization of devulcanized rubber produced using *Tulbaghia violacea* Harv. in a supercritical media. The devulcanized rubber, ranging from 5 to 35 wt% is incorporated into virgin natural rubber (NR)/styrene-butadiene rubber (SBR) blends. The effect of devulcanized rubber addition is assessed by evaluating variations in the curing characteristics, physical attributes, morphologies, mechanical properties, and dynamic mechanical analysis of several vulcanized blends. The findings indicate a reduction in the blends' curing characteristics with an increase in devulcanized rubber proportion, except for minimum torque. Furthermore, the ultimate tensile strength, elongation at break, tear strength, and rebound resilience decrease, while the tensile moduli and stiffness exhibit an increase with an increase in devulcanized rubber proportion. The observed decline in mechanical property is associated with failure points identified through surface fracture imaging. Additionally, an increase in crosslink density and hardness aligned with the alterations in dynamic mechanical properties as the proportion of devulcanized rubber is increased. The study suggests that the rubber devulcanized with *T. violacea* Harv.—when blended with virgin NR/SBR blends—could be tailored for specific applications.

1. Introduction

Waste tire management practice has a long history. The bulk of waste tires are typically stored in landfills, but they remain there for millions of years since they do not readily break down as plants or animals do.[1,2] As a result, waste tires not only take up landfill space for naturally degrading materials but also damage the linings that keep groundwater and surface water from mixing with contaminants in the landfill.[3–8] Moreover, waste tire pile fires have had a much harsher effect on the environment because they emit harmful substances, such as gases and solids, into the air, soil, and water systems.[9,10] As a result, there are significant health and safety dangers to the public from the waste tires in landfills, as well as those that have been randomly discarded. This drives researchers to develop innovative recycling methods to combat these issues. As an efficient way of recycling tires, the recovery of raw materials from waste tires has gained widespread acceptance.[7,8,10] However, current recovery processes often contribute to secondary pollution or necessitate substantial energy consumption.[1–15]

Exploring renewable resources or plant-based materials as alternative devulcanizing agents offers a promising path for more friendly recycling processes.[11–17] These materials are non-toxic and require lower temperatures and shorter reaction times for successful rubber devulcanization. For instance, Chen et al.[16] used a soybean oil-based devulcanizing agent, enhancing the compatibility and mechanical properties of the waste tire rubber/virgin rubber blends. Similarly, De et al.[15] utilized renewable resource material (RRM) to reclaim waste rubber, resulting in increased tensile moduli (at-given-elongation) but decreased ultimate tensile strength (UTS) and elongation at break (ϵ_b) as the proportion of reclaimed rubber was increased in the virgin natural rubber (NR)/styrene-butadiene rubber (SBR) blend compounds. Furthermore, Yang et al.[17] demonstrated how plant-derived lignin acted as a compatibilizer, improving the mechanical properties of the reclaimed rubber/virgin rubber blends. These examples of the usage of waste tire rubber that is devulcanized or reclaimed using plant-based materials show the same potential in promoting sustainability and reducing the environmental impact of waste tire disposal. Nevertheless, works involving rubber devulcanization or reclamation using different chemical agents often demonstrate

J. I. Mnyango, B. G. Hlangothi, B. Mabuto, S. P. Hlangothi
Centre for Rubber Science and Technology
Department of Chemistry
Nelson Mandela University
P O BOX 77000, Gqeberha 6031, South Africa
E-mail: percy.hlangothi@mandela.ac.za
C. D. Woolard
Faculty of Engineering
Stellenbosch University
Private Bag X1, Matieland, Stellenbosch 7602, South Africa

© 2024 The Authors. Macromolecular Materials and Engineering published by Wiley-VCH GmbH. This is an open access article under the terms of the Creative Commons Attribution License, which permits use, distribution and reproduction in any medium, provided the original work is properly cited.

DOI: 10.1002/mame.202300410

a detrimental effect on the final properties of recovered rubber/virgin rubber blends.

Various studies have reported differing effects of devulcanized rubber loading on the properties of devulcanized rubber/virgin rubber blends. For instance, Kojima et al.[5] noted increased Shore A hardness, tensile modulus, ϵ_b, and torque values with increasing devulcanized rubber proportion in NR/butadiene rubber blend compounds, while the optimum curing time (t_{c90}) and UTS decreased. Conversely, Mangili et al.[18] reported a reduction in maximum torque (M_H) and torque difference ($M_H - M_L$) of the devulcanized rubber/virgin rubber blend vulcanizates as the devulcanized rubber proportion increased. Jiang et al.[2] corroborated these findings. Zhao et al.[19] and Kumnuantip et al.[20] reported increased glass transition temperature (T_g), storage modulus (E'), and loss modulus (E'') but decreased maximum tangent delta (tan δ) of the devulcanized rubber/virgin rubber blend vulcanizates with increased devulcanized rubber proportion. One of the factors suggested to have contributed to the observed changes in the properties is the restriction of polymer chain mobility as more devulcanized or reclaimed rubber was added to the blends.[2,5,6,11–21]

Building upon our previous study,[13] where the crude extract of the *Tulbaghia violacea* Harv. plant exhibited devulcanizing capability on truck tire vulcanizates, our current work aims to evaluate the effect of incorporating the devulcanized rubber from that study into virgin NR/SBR blends. This was done by looking into the curing characteristics (i.e., scorch time (t_{s5}), t_{c90}, minimum torque (M_L), M_H, $M_H - M_L$, and cure rate), mechanical properties (i.e., UTS, ϵ_b, tensile moduli, tear strength, hardness, and rebound resilience), morphologies, and dynamic mechanical analysis (i.e., stiffness, E', E'', tan δ, and T_g) of the resultant vulcanizates.

2. Experimental Section

2.1. Materials and Methods

2.1.1. Rubber Compounding

Compounding materials' supplier details and preparation are the same as those in the previous work.[13] **Table 1** provides an overview of the mixing procedure followed in the preparation of unfilled and unvulcanized virgin NR/SBR blend.

The compounded NR/SBR blend was combined, according to **Table 2**, using a two-roll mill, with devulcanized rubber to get various samples, viz.: S1 to S8.[22,23] To ensure thorough blending, each sample underwent ten passes (× 10) through the mill.[22] During this process, the orientation of the sample was continuously adjusted by rotating it ≈90° between the rolls.

2.1.2. Preparation of Vulcanizates and Soxhlet Extraction

Approximately 45 g of each sample was covered with two sheets of Airbrush Stencil Mylar Film and inserted between steel plates set at 150 °C. The assembly was immediately positioned in a laboratory curing press, applying 7 MPa pressure, to initiate vulcanization at the same temperature. The cut-off time was an optimum cure time (t_{c90}), which was determined using the ASTM D6204–99 standard with the MonTech Dynamic Rubber Process Analyzer (D-RPA 3000, MDR mode), employing parameters of 0.5° oscillation angle, 1.67 Hz frequency, and 150 °C vulcanization temperature. For block-shaped samples, ≈45 g of the material was placed into a mold preheated at 150 °C, followed by curing in a press—set at 150 °C and 7 MPa—for the prescribed time (i.e., t_{c90} + 20 min). Sheeted and rectangular-shaped S1 to S8 vulcanizates were conditioned under ambient conditions for 72 h before conducting any tests. The Soxhlet extraction was performed following the procedures detailed in the previous work,[13] employing the same set of solvents and justifications.

Table 1. Rubber compounding procedure.

Step	Action
	Mixing of virgin rubbers
1	70 phr NR and 30 phr SBR were blended using a two-roll mill, forming the NR/SBR raw blend.
	First-stage
2	This blend was further mixed for 1 min at 80 rpm in the internal mixer.
3	Zinc oxide (5 phr) and stearic acid (2 phr) were added to the blend in the internal mixer and mixed at 80 rpm for 3 min. Renacit 7 (0.1 phr) and *N*-(1,3-dimethylbutyl)-*N*′-phenyl-p-phenylenediamine (5 phr) were then added simultaneously, followed by blending for an additional 3 min at 80 rpm. To moderate the temperatures caused by the high internal friction at 80 rpm, the mixing speed was reduced to 60 rpm before adding paraffinic oil (10 phr) and polyethylene glycol 4000 (0.5 phr), which were then blended for another 3 min.
4	The rubber compound obtained after step 3 was removed from the internal mixer and sheeted (×2) on a two-roll mill.
	Second-stage
5	The sheeted rubber compound was loaded into the internal mixer and mixed with sulfur (1.5 phr) and *N*-cyclohexylbenzothiazol-2-sulphenamide (1 phr) simultaneously for 3 min at 40 rpm.

2.1.3. Characterization of Devulcanized Rubber

Table 3 shows the characteristics of the devulcanized rubber, where the parameters were measured using a simultaneous differential scanning calorimetry-thermogravimetric analyzer (SDT Q600 from TA Instruments, United States), whose temperature was calibrated using a high-purity zinc standard's melting en-

Table 2. Incorporation of devulcanized rubber into unfilled and unvulcanized virgin NR/SBR blend compounds.

Virgin NR/SBR blend compound [wt%]	Devulcanized rubber [wt%]	Designation
100	0	S1
95	5	S2
90	10	S3
85	15	S4
80	20	S5
75	25	S6
70	30	S7
65	35	S8

© 2024 The Authors. Macromolecular Materials and Engineering published by Wiley-VCH GmbH

Table 3. Characteristics of devulcanized rubber obtained using SDT.

Parameter	Weight [wt%]
Volatiles	7.2
Polymers	56.6
Carbon black	31.8
Inorganics	3.7

dotherm. A sample of ≈10 mg in an alumina crucible (90 µL) was heated at a rate of 5 °C min^{-1} from ambient temperature to 800 °C in a nitrogen atmosphere flowing at 100 mL min^{-1} through the balance, with a switch—done promptly after cooling—of purge gas to oxygen at 550 °C. Runs were repeated in triplicates; reported in Table 3 are average values.

2.2. Analyses

2.2.1. Determination of Curing Characteristics

A D-RPA 3000 was used (in MDR mode) to determine the curing characteristics of S1 to S8 shown in Table 2, employing parameters of 0.5° oscillation angle, 1.67 Hz frequency, and 150 °C temperature. The scorch time (t_{s5}), minimum torque (M_L), maximum torque (M_H), torque difference ($M_H - M_L$), and cure rate were the curing characteristics studied in addition to t_{c90}.

2.2.2. Swelling Tests

The swelling tests for determining the crosslink densities of S1 to S8 vulcanizates were carried out as reported in the previous work.[13] Since S2 to S8 contained carbon black (CB) filler, their rubber volume fraction (V_r) was corrected by Kraus equations (Equation (1))[7]

$$V_{r0}/V_r = 0.56^{-z} + 0.44 \tag{1}$$

where, V_{r0} is the corrected volume fraction of the rubber network in the swollen gel, and z is the mass concentration of CB filler.

2.2.3. Measurement of Mechanical Properties

Tensile Properties: A Benchmaster cutter from Sterling Machinery Exchange (South El Monte, United States) was used to punch out tensile test specimens in accordance with ASTM D638 type IV standard dumbbell die. Using a Fowler Ultra-Cal V Electronic Caliper (6″/150 mm), the specimens' thickness (2 mm) and width (6 mm) were measured. Tinius Olsen tensile tester (Noida, India) equipped with a load cell of 5 kN was used to measure the tensile properties at ambient temperature as per ASTM D412-06a. The crosshead speed was set to 500 mm min^{-1}, and the sample rate was 10 pts s^{-1}. An extensometer by Tinius Olsen with a 25 mm travel gauge was used. Data for modulus at 100% (M100), 200% (M200), and 300% (M300) elongation, as well as UTS and elongation at break (ϵ_b), were recorded. Each set of samples had six specimens, and the average results were utilized to determine their respective final values.

Tear Strength: The specimens for tear resistance or strength testing were cut out according to ASTM D624 Type C (right angle) test piece type. Based on the same standard test, the Universal Tensile Testing Tensometer (Shimadzu, Japan) was used at 20 mm min^{-1} with 1 kN load cell. The test specimens were 2 mm thick, 10 mm wide, and had a length of 102 mm. To get the tear strength values, the highest rupture force was determined and divided by the thickness of the test specimen.[24] For each set of samples, six specimens were used, and average values were given.

Hardness: The hardness property—type Shore A—of rectangular-shaped samples of 50 mm × 25 mm × 25 mm (length × width × thickness) was examined. The test was performed in accordance with ASTM D2240 on a Durometer (Hildebrand Prüf- und Meßtechnik GmbH, Germany). It was done by setting a sample on the instrument's flat surface underneath its indenter and then using the instrument's manually operated lever to allow the indenter to press onto the sample.[22] Following 5 s of solid contact between the indenter and the sample, the hardness was determined.[22] Values were acquired at three separate positions on the sample's smooth sides during testing at room temperature.[22] These values were then averaged, and the resultant figures were recorded.

Rebound Resilience: A vertical rebound pendulum (Scott) was used to measure in accordance with ASTM D2632-01 the rebound resilience (R, %) of samples similar to those tested for hardness. The testing was done at ambient temperature. After inserting the test block into the instrument's holder, the pendulum's arm was permitted to descend at 15° (angle of incidence), striking the test block's midsection.[22] The three readings' average was used as one data point.[22] R was measured utilizing Equation (2) in accordance with ASTM D2632-01

$$R\,\% = \frac{1 - \cos\left(\text{angle of rebound}\right)}{1 - \cos\left(\text{angle of incidence}\right)} \times 100 \tag{2}$$

2.2.4. Morphological Properties

Examination of the tensile fractured surfaces was performed using a JSM-IT100 InTouchScope scanning electron microscope (SEM, JEOL Ltd., Tokyo, Japan). For superior image resolution and to prevent electrostatic charging on sample surfaces, gold was sputtered-coated onto them before analysis.[24] A mix of two signals (i.e., backscattered electron detector [BSD] and secondary electron detector [SED]), an accelerating voltage of 10 kV, and a working distance of 11 mm were employed for the examination.

2.2.5. Dynamic Mechanical Analysis

Dynamic mechanical properties of S1 to S8 vulcanizates, viz.: stiffness, storage modulus (E'), loss modulus (E''), tangent delta (tan δ) and glass transition temperature (T_g), were determined using a TA instrument Q800 (New Castle, United States) dynamic mechanical analyzer (DMA). Rectangular specimens with dimensions of 13 mm × 7 mm × 2 mm (length × width × thickness) underwent tension mode analysis (DMA Multi-frequency-strain) utilizing a film tension clamp measuring system.[20] Prior

© 2024 The Authors. Macromolecular Materials and Engineering published by Wiley-VCH GmbH

Table 4. Effect of devulcanized rubber percentage on the curing properties of various samples.

Sample	t_{s5} [min]	t_{c90} [min]	M_L, [dNm]	M_H [dNm]	$M_H - M_L$ [dNm]	Cure rate [dNm min^{-1}]
S1	14.2	18.5	0.8	7.3	6.5	1.8
S2	13.5	18	0.7	7.2	6.5	1.8
S3	13	16.5	0.7	6.8	6.2	1.7
S4	12.6	14.9	0.7	6.6	5.9	1.6
S5	11.9	14.5	0.8	6.5	5.7	1.5
S6	10.8	14	0.8	6.1	5.3	1.3
S7	10.6	13.6	0.9	5.8	4.9	1
S8	6.1	13.4	1.1	6.1	5	0.8

to the tests, calibration was performed for the film tension and clamp compliance (<0.5 µm N^{-1}). Specimens were subjected to a set strain (10.00%), frequency (1.00 Hz), and preload force (0.0100 N). The analysis was conducted over a temperature range of −80 to +60 °C using liquid nitrogen—as a cooling system—and a heating rate of 5.00 °C min^{-1}.[20]

3. Results and Discussion

3.1. Characterization of Blends

3.1.1. Curing Characteristics

The changes in the cure characteristics presented in **Table 4** align with findings from prior studies.[16,25–35] As the proportion of devulcanized rubber increased, an overall decrease in the cure characteristics of the blends was observed. This is because the devulcanized rubber contains a lesser number of active cure sites, pendant groups from residual crosslinks, and shorter rubber chains due to chain scission during devulcanization processes, compared to the virgin counterparts.[32,36–43] Consequently, this results in reduced processability as more of the virgin rubber is replaced by the devulcanized rubber. The notable decrease in both scorch time (t_{s5}) and optimum cure time (t_{c90}) can be attributed to crosslink precursors in devulcanized rubber and the presence of active crosslinking sites, facilitating crosslinking upon heating. A slight increase in minimum torque (M_L) was observed for blends containing 20 wt% ≤ devulcanized rubber loading (i.e., S2 to S5). This marginal rise in M_L can be attributed to the presence of CB filler and the existence of crosslinks within the devulcanized rubber, which tends to elevate stock viscosity.[29,30,32,35–43] At and beyond 25 wt% devulcanized rubber loading (i.e., S6 to S8), t_{c90} stabilizes, likely due to the crosslinked state of devulcanized rubber limiting further crosslink formation in the blends.

3.1.2. Crosslink Density

Increases in the devulcanized rubber proportion in the blends resulted in corresponding increases in the crosslink densities (**Figure 1**). This is primarily due to the presence of residual crosslinks in the devulcanized rubber that adds to the existing crosslink density. During devulcanization, some crosslinks persist in the rubber while others are severed.[10,32,37,38] These residual crosslinks from the devulcanized rubber therefore contribute to the overall crosslink density of the blend upon re-vulcanization to form new blends. Furthermore, the devulcanized rubber also has some available active or functional sites that can undergo vulcanization, crosslinking with the virgin rubber chains thereby forming additional crosslinks.[44–46] Additionally, increases in the crosslink densities of the blends as the devulcanized rubber proportion increased is demonstrated by corresponding increases in hardness and stiffness of the blends while elongation at break (ϵ_b) decreases (Sections 3.1.3 and 3.1.5).

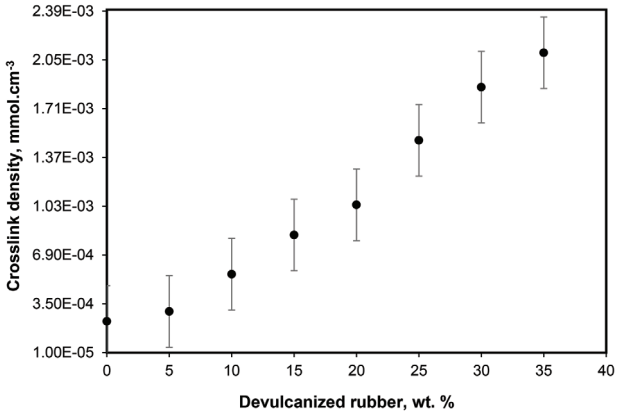


Figure 1. Effect of devulcanized rubber percentage on the crosslink density of various vulcanizates.

3.1.3. Mechanical Properties

Tensile properties: It is apparent from **Figures 2** and **3** that the addition of the devulcanized rubber is detrimental to the UTS and elongation at break (ϵ_b) of the blends. This is revealed by a decline in these tensile properties as the devulcanized rubber loading is increased. This reduction can be explained by the existence of residual crosslinks in the devulcanized rubber, which affect compatibility with the virgin rubbers. Residual crosslinks in the devulcanized rubber result in poor mixing, entanglements,

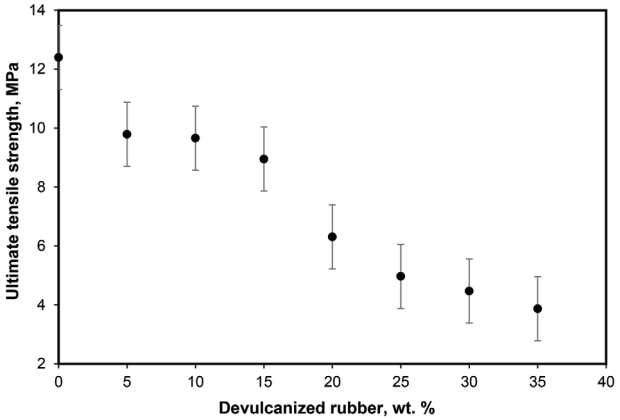


Figure 2. Effect of devulcanized rubber percentage on the ultimate tensile strength of various vulcanizates.

© 2024 The Authors. Macromolecular Materials and Engineering published by Wiley-VCH GmbH

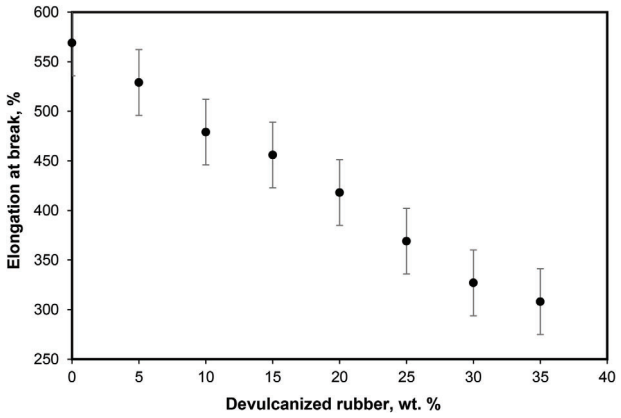


Figure 3. Effect of devulcanized rubber percentage on the elongation at break of various vulcanizates.

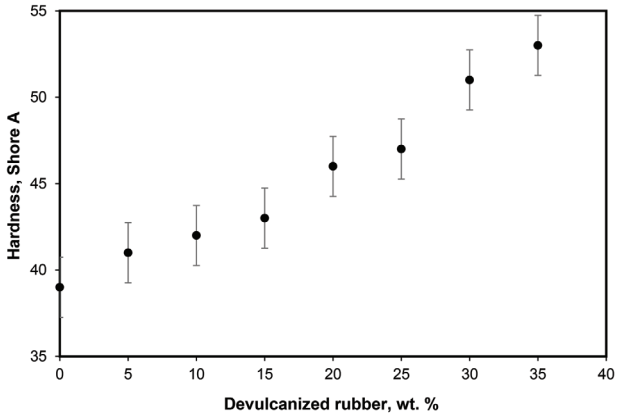


Figure 5. Effect of devulcanized rubber percentage on the hardness of various vulcanizates.

and crosslinking of this devulcanized rubber with the virgin rubber chains.[47–50] This results in poor interfacial adhesion, creating weak interfaces that can act as sites for stress concentration and initiation of cracks, thereby reducing vulcanizates' ability to effectively transfer stress. Consequently, the UTS and ϵ_b are reduced.[18,27,36,47,51] Similarly, the devulcanized rubber may contain remnant devulcanizing agents, by-products, or pendant groups that may interfere with the polymer network, reducing its strength and elasticity.[15,18,27,32]

Increases in the tensile moduli of the blends (**Figure 4**) with increased devulcanized rubber proportion indicate increases in the stiffness of these blends. This is mainly attributed to increased restriction in the movement of polymer chains as the devulcanized rubber proportion is increased. Restriction in rubber chain mobility impedes its ability to deform under applied stress, resulting in higher stiffness or modulus. Research by Ismail et al.[31] suggests that the heightened modulus of blends with increased devulcanized rubber proportion implies the behavior of the utilized devulcanized rubber as a rigid particulate filler, inducing stiffness and thereby augmenting the modulus. Similarly, increases in the devulcanized rubber proportion also increase the CB filler content, which, due to its reinforcing ability, results in reduced rubber chain mobility thereby enhancing stiffness. Additionally, during devulcanization processes, main chain scission may occur alongside crosslink scission, resulting in shorter rubber chains that tend to increase the overall stiffness of the blends.[5,12,15,18,19,25,27,32,42,45–48] Moreover, as observed in Figure 1, the addition of the devulcanized rubber increases the crosslink density of the blends due to residual crosslinks in the devulcanized rubber. These additional crosslinks further enhance the stiffness of the blends by retarding molecular chain mobility, resulting in a greater load being needed for elongation, thereby increasing the overall tensile moduli of the blends.[15,31,39,46,50,52]

Tear Strength, Hardness, and Rebound Resilience: Increases in blends' hardness (**Figure 5**) with increased devulcanized rubber proportion corroborate the observed increases in the crosslink densities (Figure 1). This notable increase in crosslink density, as well as increased stiffness and CB filler content, associated with higher devulcanized rubber loading significantly contributes to the increased hardness of the blends, as depicted in Figure 5. Conversely, the reduced compatibility associated with the devulcanized rubber due to residual crosslinks as explained before, results in failure points that hinder effective stress transfer in the blends. Consequently, reductions in the tear strength (**Figure 6**) and rebound resilience (**Figure 7**) of the blends are observed as the devulcanized rubber proportion is increased. Furthermore,

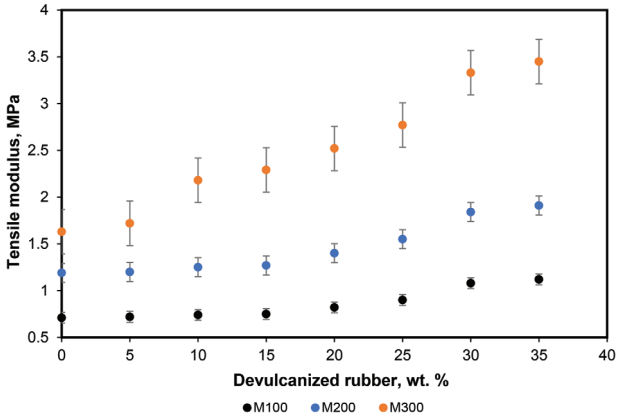


Figure 4. Effect of devulcanized rubber percentage on the tensile modulus at 100%, 200%, and 300% elongation of various vulcanizates.

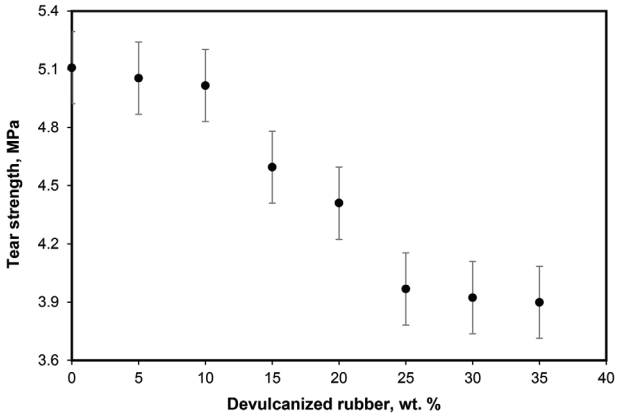


Figure 6. Effect of devulcanized rubber percentage on the tear strength of various vulcanizates.

© 2024 The Authors. Macromolecular Materials and Engineering published by Wiley-VCH GmbH

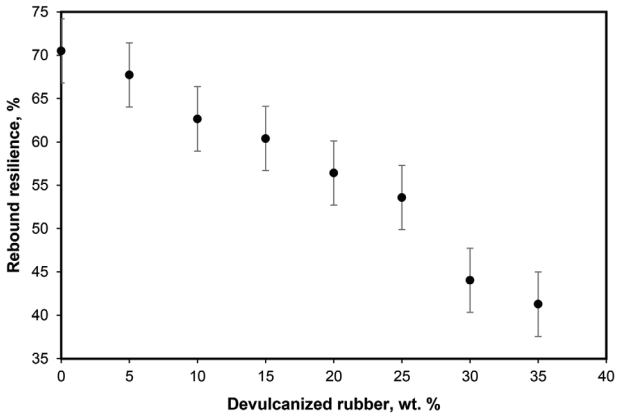


Figure 7. Effect of devulcanized rubber percentage on the rebound resilience of various vulcanizates.

the devulcanization process alters the molecular structure and chain length of the rubber, subsequently influencing characteristics like elasticity and its ability to effectively interact with the virgin counterpart.[30,43,45] These changes in the rubber chain structure hinder the material's capability to regain its original form after deformation, thereby diminishing its rebound resilience. Consequently, the introduction of increasing amounts of devulcanized rubber leads to an overall decline in the elasticity and resilience of the blends.

3.1.4. Morphological Properties

The surface morphology of S1 (i.e., 100 wt% virgin rubber vulcanizate) shows homogeneity with featureless fractal texture (**Figure 8a**).[23,24,53] This pattern often denotes the vulcanizate's superior mechanical strength and resistance to failure,[23,24,31,32,51,53] which was previously shown under mechanical properties. The blends comprising 5, 10, and 15 wt% devulcanized rubber, which are S2, S3, and S4 vulcanizate, respectively, exhibited a similar pattern (Figures 8b–d), though the latter two (i.e., S3 and S4 vulcanizates) showed minimal micro defects (yellow arrow). This similarity in patterns between S1 vulcanizate and S2 to S4 vulcanizates suggests that the devulcanized rubber is evenly distributed throughout the matrix with good compatibility.[16,23,24,31,32,34,51] Shown by Figure 8e–g, however, is that as the devulcanized rubber proportion increased further (≥ 20 wt%), featured regions appeared as a result of numerous holes (black arrow) and cracked paths (red arrow). These regions show points of defects that are the root of the lowering of mechanical properties or failure of the blends. The defects substantially weaken the interaction between the devulcanized rubber and virgin rubber matrix resulting in poor interphase strength thereby rendering the blends susceptible to failure via detachment of devulcanized rubber from the virgin rubber matrix.[16,23,31,32,45,54,55] Consequently, the blends with ≥ 20 wt% devulcanized rubber proportion (i.e., S5 to S8 vulcanizates) had considerably inferior UTS, ϵ_b, and tear strength.

3.1.5. Dynamic Mechanical Analysis

The stiffness and storage modulus results were determined at the temperature (i.e., −80 °C) at which all runs were set to end, whereas the loss modulus results were determined at the temperature (i.e., −50 °C) at which the samples showed their peaks' maximum point.[20] **Figure 9** shows the effect of devulcanized rubber loading on the stiffness (i.e., dynamic rigidity of a material) as a function of test temperature for S1 to S8 vulcanizates. It increased substantially with the proportion of devulcanized rubber. According to previous research,[20,26,55] this increase in stiffness is caused by restricted polymer chain mobility, resulting from increased crosslink density and CB filler content that is due to increased devulcanized rubber proportion in the vulcanizates. Figure 1 demonstrates how the devulcanized rubber loading increased the crosslink density of the S1 to S8 vulcanizates. As a result of increasing stiffness, the storage modulus (E') increased (**Figure 10**), the outcomes found to be consistent with those of the tensile moduli (Figure 4). Additionally, E' is the material's elastic response, which explains why it increased as stiffness increased.[20,24,27,32] A comparable trend was seen with loss modulus (E'') (**Figure 11**), which is the amount of heat or energy lost through internal friction and motion over the course of one load cycle.[32] Typically, E'' measures the viscous component's dissipated energy, that is, energy that cannot be recovered during a load cycle.[17,20,22,24,27,32] In addition to stiffness, E'' increased because of increased internal molecular friction and viscoelasticity of the vulcanizates, which resulted from increased crosslink density and CB filler content associated with increased devulcanized rubber proportion.[16,20,23,24,26,27,29,32,45]

Table 5. Effect of devulcanized rubber percentage on the tangent delta and glass transition temperature of various vulcanizates.

Sample	tan δ	T_g [°C]
S1	1.3	−34
S2	1.2	−34
S3	1.1	−31
S4	1.1	−30
S5	1	−29
S6	1	−29
S7	0.9	−28
S8	0.7	−25

A further parameter assessed from the dynamic mechanical analysis of S1 to S8 vulcanizates was the maximum tangent delta (tan δ), which was utilized to determine the glass transition temperature (T_g) of these vulcanizates. Similar to those reported by Kumnuantip et al.,[20] the tan δ values of the vulcanizates were found to decrease while their T_g increased as the devulcanized rubber proportion increased (**Table 5**). These results can be attributed to the same reasons that induced stiffness, E', and E''.[20,24,52] Furthermore, the tan δ values of S2 to S8 vulcanizates were anticipated to be lower than tan δ value of S1 vulcanizate since CB itself has a very low loss angle.[20,24,44,45,56] Therefore, a considerable reduction in the values of tan δ suggested a relatively high interaction between CB (in the devulcanized rubber) and virgin rubber matrix.[20,56] Thus, the observed properties that are typically influenced by CB filler including M_L, crosslink density, UTS, ϵ_b, tensile moduli, tear strength, E', E'', and T_g.[20,24,44,45,52,56]

© 2024 The Authors. Macromolecular Materials and Engineering published by Wiley-VCH GmbH

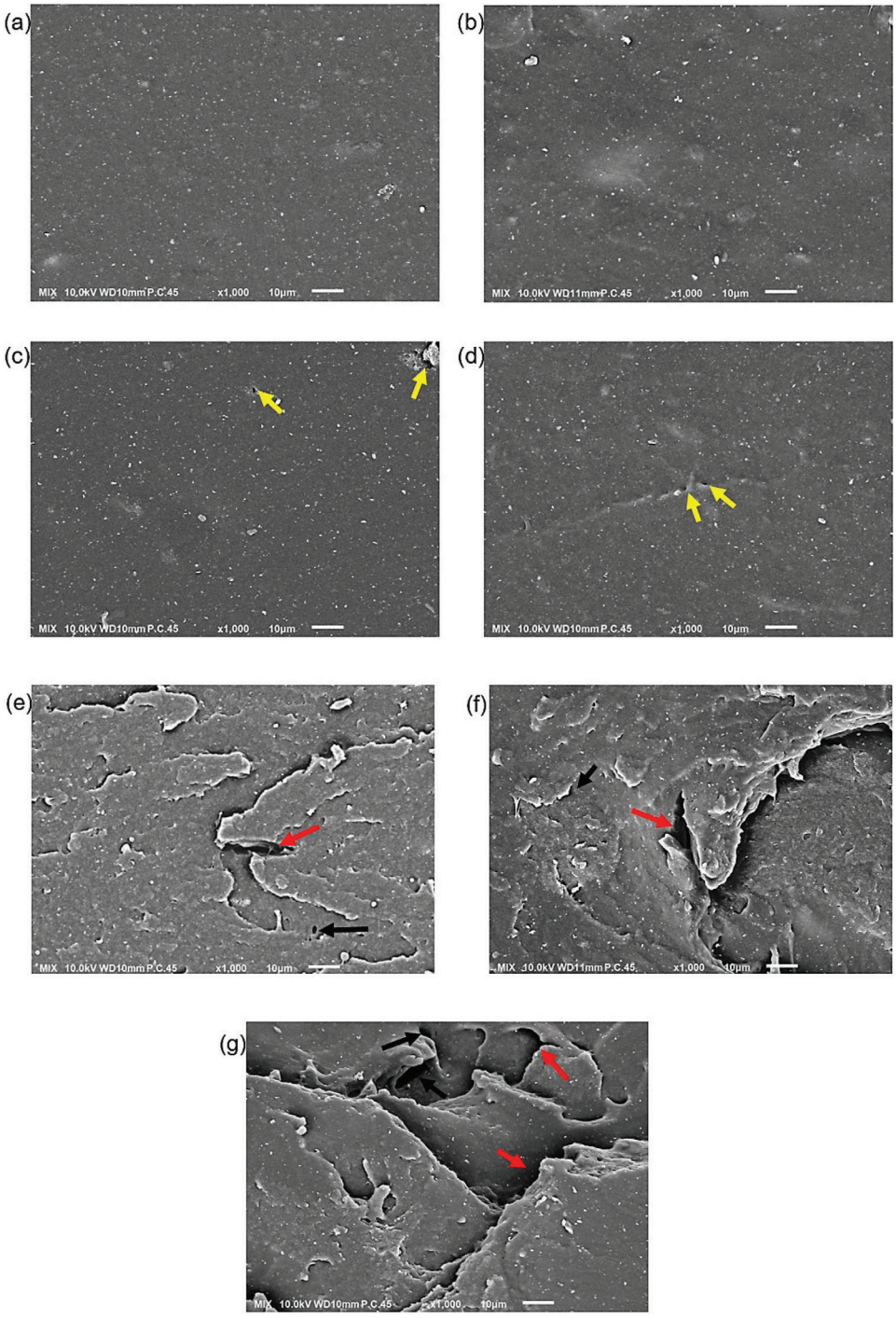


Figure 8. Tensile fractured surfaces of different vulcanizates: a) 0, b) 5, c) 10, d) 15, e) 20, f) 30, and g) 35 wt% devulcanized rubber loading.

4. Conclusion

The incorporation of devulcanized rubber in virgin natural rubber/SBR blends resulted in a decrease in UTS, tear strength, elongation at break, and rebound resilience, while the crosslink density, tensile moduli, hardness, and most of the dynamic mechanical properties exhibited an increase. The decrease in the former was attributed to the presence of residual crosslinks in the devulcanized rubber, as indicated by a reduction in most of the blends' curing characteristics. Notably, the variations in UTS revealed an optimal devulcanized rubber content of 15 wt%, where further additions demonstrated detrimental effects. Moreover, the blend containing this devulcanized rubber content demonstrated only a marginal decline of 3.5 MPa in UTS, highlighting the potential use of the examined devulcanized rubber in rubber formulations without significantly compromising the tensile

 © 2024 The Authors. Macromolecular Materials and Engineering published by Wiley-VCH GmbH

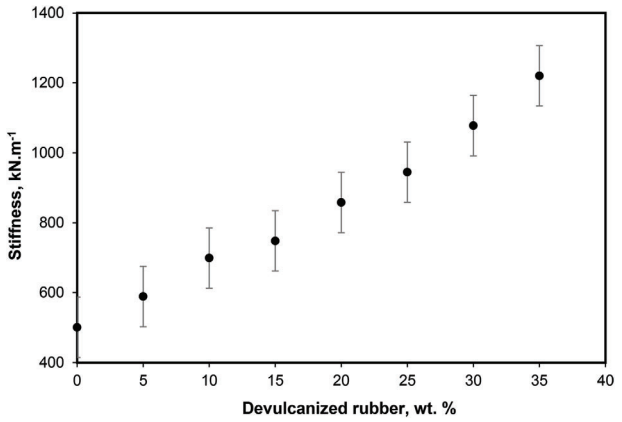


Figure 9. Effect of devulcanized rubber percentage on the stiffness of various vulcanizates.

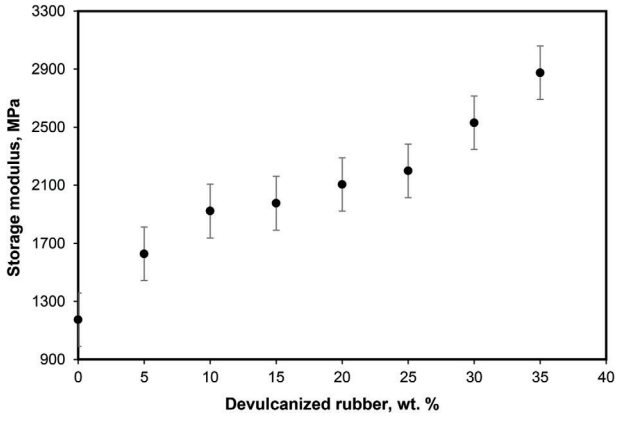


Figure 10. Effect of devulcanized rubber percentage on the storage modulus of various vulcanizates.

strength. Consequently, the investigation illustrates the viability of *T. violacea* Harv. extract as an eco-friendly yet efficient potential devulcanizing agent, which could be readily employed for industrial applications owing to its renewability and natural abundance, thereby facilitating the manufacturing of cost-effective products.

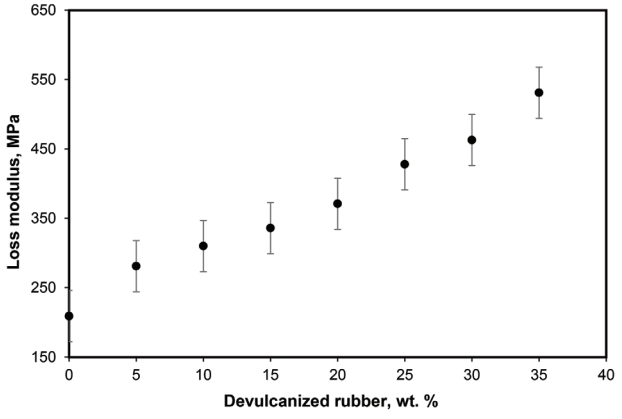


Figure 11. Effect of devulcanized rubber percentage on the loss modulus of various vulcanizates.

Acknowledgements

This work was financially supported by both the National Research Foundation Scholarship and the Nelson Mandela University Postgraduate Research Scholarship.

Conflict of Interest

The authors declare no conflict of interest.

Data Availability Statement

The data that support the findings of this study are available on request from the corresponding author. The data are not publicly available due to privacy or ethical restrictions.

Keywords

devulcanization, devulcanized rubber, pneumatic truck tire, rubber properties, rubber recycling, *Tulbaghia violacea*

Received: November 16, 2023
Revised: January 25, 2024
Published online: February 23, 2024

[1] M. Kojima, K. Ogawa, H. Mizoshima, M. Tosaka, S. Kohjiya, Y. Ikeda, *Rubber Chem. Technol.* **2003**, *76*, 957.
[2] K. Jiang, J. Shi, Y. Ge, R. Zou, P. Yao, X. Li, L. Zhang, *J. Appl. Polym. Sci.* **2013**, *127*, 2397.
[3] L. Asaro, M. Gratton, N. Poirot, S. Seghar, N. Ait Höcine, *Waste Manage.* **2020**, *118*, 647.
[4] M. Kojima, M. Tosaka, Y. Ikeda, *Green Chem.* **2004**, *6*, 84.
[5] M. Kojima, M. Tosaka, Y. Ikeda, S. Kohjiya, *J. Appl. Polym. Sci.* **2005**, *95*, 137.
[6] I. Mangili, E. Collina, M. Anzano, D. Pitea, M. Lasagni, *Polym. Degrad. Stab.* **2014**, *102*, 15.
[7] Z. Liu, X. Li, X. Xu, X. Wang, C. Dong, F. Liu, W. Wei, *Polym. Degrad. Stab.* **2015**, *119*, 198.
[8] X. Li, X. Q. Deng, C. Dong, *J. Braz. Chem. Soc.* **2018**, *29*, 2169.
[9] M. Kojima, S. Kohjiya, Y. Ikeda, *Polymer* **2005**, *46*, 2016.
[10] L. Bockstal, T. Berchem, Q. Schmetz, A. Richel, *J. Cleaner Prod.* **2019**, *236*, 117574.
[11] P. Song, C. Wan, Y. Xie, K. Formela, S. Wang, *Waste Manage.* **2018**, *78*, 238.
[12] Y. Xie, A. A. Hassan, P. Song, Z. Zhang, S. Wang, *Polym. Degrad. Stab.* **2019**, *167*, 292.
[13] J. I. Gumede, B. G. Hlangothi, B. Mabuto, C. D. Woolard, S. P. Hlangothi, *J. Cleaner Prod.* **2022**, *362*, 132478.
[14] J. I. Gumede, B. G. Hlangothi, C. D. Woolard, S. P. Hlangothi, *Waste Manage. Res.* **2021**, *40*, 490.
[15] D. De, S. Maiti, B. Adhikari, *J. Appl. Polym. Sci.* **2000**, *75*, 1493.
[16] L. Chen, Q. Zhao, L. Zhang, *J. Appl. Polym. Sci.* **2018**, *135*, 46366.
[17] J. Yang, Y. Meng, J. Zhang, H. Xu, J. Yu, X. Li, *J. Appl. Polym. Sci.* **2015**, *132*, 41422.
[18] I. Mangili, M. Lasagni, M. Anzano, E. Collina, V. Tatangelo, A. Franzetti, P. Caracino, A. I. Isayev, *Polym. Degrad. Stab.* **2015**, *121*, 369.
[19] X. Zhao, H. Hu, D. Zhang, Z. Zhang, S. Peng, Y. Sun, *e-Polymers* **2019**, *19*, 482.
[20] C. Kumnuantip, N. Sombatsompop, *Mater. Lett.* **2003**, *57*, 3167.

 © 2024 The Authors. Macromolecular Materials and Engineering published by Wiley-VCH GmbH

[21] L. A. Rios, D. S. Rosa, L. A. Pessan, *Mater. Res.* **2015**, *18*, 136.
[22] J. I. Gumede, M.Sc. Thesis, Nelson Mandela University, Port Elizabeth, South Africa **2019**.
[23] S. Ghoria, S. Bhunia, M. Roy, D. De, *Polym. Degrad. Stab.* **2016**, *129*, 34.
[24] S. Ramarad, Ph.D. Thesis, University of Nottingham, Nottingham, England **2016**.
[25] D. De, D. De, G. M. Singharoy, *Polym. Eng. Sci.* **2007**, *47*, 1091.
[26] S. Rooj, G. C. Basak, P. K. Maji, A. K. Bhowmick, *J. Polym. Environ.* **2012**, *19*, 382.
[27] E. Abraham, B. M. Cherian, P. A. Elbi, L. A. Pothen, S. Thomas, in, *Recent Developments in Polymer Recycling*, (Eds., A. Fainleib, O. Grigoryen), Transworld Research Network, Kerala, India **2011**, pp. 47–100.
[28] V. Rek, H. J. Mencer, M. Bravar, *Polym. Photochem.* **1986**, *7*, 273.
[29] T. D. Sreeja, S. K. N. Kutty, *Polym.-Plast. Technol. Eng.* **2000**, *39*, 501.
[30] H. Ismail, R. Nordin, A. M. Noor, *Iran. Polym. J.* **2003**, *12*, 373.
[31] H. Ismail, R. Nordin, A. M. Noor, *Polym. Test.* **2002**, *21*, 565.
[32] S. Ramarad, M. Khalid, C. T. Ratnam, A. L. Chuah, W. Rashmi, *Prog. Mater. Sci.* **2015**, *72*, 100.
[33] D. De, D. De, B. Dey, S. C. Debnath, B. C. Roy, *Eur. Polym. J.* **2006**, *42*, 917.
[34] H. M. Costa, V. D. Ramos, *Polym. Test.* **2008**, *27*, 27.
[35] J. I. Gumede, J. Carson, S. P. Hlangothi, L. L. Bolo, *Mater. Today Commun.* **2020**, *23*, 100852.
[36] T. D. Sreeja, S. K. N. Kutty, *Int. J. Polym. Mater.* **2003**, *52*, 599.
[37] S. Li, J. Lamminmäki, K. Hanhi, *J. Appl. Polym. Sci.* **2005**, *97*, 208.
[38] X. Zhang, C. Lu, M. Liang, *J. Polym. Res.* **2009**, *16*, 411.
[39] T. D. Sreeja, S. K. N. Kutty, *J. Elastomers Plast.* **2002**, *34*, 145.
[40] D. A. Simon, D. Pirityi, P. Tamás-Bényei, T. Bárány, *J. Appl. Polym. Sci.* **2020**, *137*, 48351.
[41] D. A. Simon, D. Z. Pirityi, T. Bárány, *Sci. Rep.* **2020**, *10*, 16587.
[42] N. S. S. Saimi, S. N. L. Mamauod, N. A. Majid, S. S. Sarkawi, Z. Z. Abidin, *AIP Conf. Proc.* **2021**, *2339*, 020116.
[43] D. A. Simon, T. Bárány, *Polym. Degrad. Stab.* **2021**, *190*, 109626.
[44] Ł. Zedler, D. Kowalkowska-Zedler, X. Colom, J. Cañavate, M. R. Saeb, K. Formela, *Polymers* **2020**, *12*, 3018.
[45] D. De, P. K. Panda, M. Roy, S. Bhunia, *Mater. Des.* **2013**, *46*, 142.
[46] N. Sombatsompop, C. Kumnuantip, *J. Appl. Polym. Sci.* **2003**, *87*, 1723.
[47] D. T. Farahani, G. R. Bakhshandeh, M. Abtahi, *Polym. Bull.* **2006**, *56*, 495.
[48] J. Lamminmäki, S. Li, K. Hanhi, *J. Mater. Sci.* **2006**, *41*, 8301.
[49] M. Balasubramanian, *J. Polym. Res.* **2009**, *16*, 133.
[50] N. Rattanasom, A. Poonsuk, T. Makmoon, *Polym. Test.* **2005**, *24*, 728.
[51] D. De, D. De, *Mater. Sci. Appl.* **2011**, *2*, 486.
[52] C. T. Hiranobe, G. D. Ribeiro, G. B. Torres, E. A. P. dos Reis, F. C. Cabrera, A. E. Job, L. L. Paim, R. J. dos Santos, *Mater. Res.* **2021**, *24*.
[53] L. Velisavljević, J. H. Elder, *Vision Res.* **2006**, *46*, 2166.
[54] Y. Li, S. Zhao, Y. Wang, *Polym. Degrad. Stab.* **2011**, *96*, 1662.
[55] Y. Li, S. Zhao, Y. Wang, *J. Polym. Environ.* **2012**, *20*, 372.
[56] P. P. A. Smit, *Rheol. Acta* **1966**, *5*, 277.

 © 2024 The Authors. Macromolecular Materials and Engineering published by Wiley-VCH GmbH